Biosensors and Bioelectronics 35 (2012) 128–133

Contents lists available at SciVerse ScienceDirect

Biosensors and Bioelectronics

journal homepage: www.elsevier.com/locate/bios

A study of electrochemical biosensor for analysis of three-dimensional (3D) cell culture

Se Hoon Jeong[a,*], Dong Woo Lee[a], Sanghyo Kim[b], Jhingook Kim[c], Bosung Ku[a,**]

[a] Advanced Materials & Devices Lab, Corporate R&D Institute, Samsung Electro-Mechanics Co., Ltd., Suwon 443-743, Republic of Korea
[b] College of Bionano technology, Gachon University, Seongnam 461-701, Republic of Korea
[c] Samsung Medical Center, School of Medicine, Sungkyunkwan University, Seoul 135-230, Republic of Korea

ARTICLE INFO

Article history:
Received 25 November 2011
Received in revised form 7 February 2012
Accepted 15 February 2012
Available online 25 February 2012

Keywords:
Cell chip
Three-dimensional (3D) cell culture
Electrochemical biosensor
Electrical conductivity
Cytotoxicity assay

ABSTRACT

Cell culture has a fundamental role not only in regenerative medicine but also in biotechnology, pharmacology, impacting both drug discovery and manufacturing. Although cell culture has been generally developed for only two-dimensional (2D) culture systems, three-dimensional (3D) culture is being spotlighted as the means to mimic in vivo cellular conditions. In this study, a method for cytotoxicity assay using an electrochemical biosensor applying 3D cell culture is presented. In order to strengthen the advantage of a 3D cell culture, the experimental condition of gelation between several types of sol–gels (alginate, collagen, matrigel) and cancer cells can be optimized to make a 3D cell structure on the electrode, which will show the reproducibility of electrical measurement for long-term monitoring. Moreover, cytotoxicity test results applying this method showed IC_{50} value of A549 lung cancer cells to erlotinib. Thus, this study evaluates the feasibility of application of the electrochemical biosensor for 3D cell culture to cytotoxicity assay for investigation of 3D cell response to drug compounds.

1. Introduction

Generally, a cell-based biosensor has been developed for only two-dimensional (2D) culture systems. Although some drug compounds are effective in vitro, they might not be effective in vivo because of the difference between in vitro and in vivo conditions. Since a 2D culture forming mono layer has contact inhibition among cells and might change the original characteristic of cell morphology and functionality, unlike three-dimensional (3D) cultures forming multi layers (Mueller-Klieser, 1997; Petersen et al., 1992). 3D cell models, however, can mimic in vivo cellular conditions because they have a 3D scaffold that supports cell growth and cell functions including morphogenesis, cell metabolism and cell-to-cell interactions (Lee et al., 2008a; Yang et al., 2008). For these reasons, optimization of the experimental condition in the scaffold matrix of 3D cell cultures is needed to develop a biosensor for cytotoxicity assay on 3D cell culture.

Currently, optical detectors have been used as a commercial analytical bio-device to observe cell responses, although they remain expensive due to their high-cost modules and fluorescent materials. They also have experimental limitations because they, like most optical devices, are not portable size. On the other hand, electrical detection systems have unique advantages such as simultaneous real-time analysis, high-cost efficiency, versatile fabrication, label-free biosensors, and portable-size devices and simply operated analytical instruments (Albers et al., 2003; Mehrvar and Abdi, 2004; Jeong et al., 2009). Based on the advantages, electrochemical techniques are a powerful tool that can be applied when studying the cell immobilization, adhesion, proliferation and apoptosis (Ding et al., 2007). Moreover, electrochemical detection systems provide precise and real-time information of cell status by monitoring of metabolic compounds in cell cultures, such as glucose, lactate and oxygen to deeply understand the mechanisms of various types of cells (Boero et al., 2011; Zhang et al., 2011; Rodrigues et al., 2008; Kaya et al., 2003). Recently, by combining the electrochemical detection systems with nanoscale materials, nanostructured biosensors have been developed in order to overcome detection limit and improve sensitivity (Boero et al., 2011). Furthermore, multi-channel measurement systems are capable of real-time monitoring which can be effectively used in drug discovery as a high-throughput screening method (Yue et al., 2008; Andreescu and Sadik, 2005).

In this study, our current work addresses the development of a novel electrochemical biosensor for cytotoxicity assay on 3D cell culture that combines the advantages mentioned above. Although the common electrochemical biosensor has a unique advantage of being able to measure cell signals in real time unlike optical biosensors, its process of measuring accurate electrical signals from

* Corresponding author. Tel.: +82 31 218 2217; fax: +82 31 210 6329.
** Corresponding author. Tel.: +82 31 210 5463.
E-mail addresses: sehoon.jeong@samsung.com, jeongsh422@gmail.com (S.H. Jeong), bosung.ku@samsung.com (B. Ku).

0956-5663/$ – see front matter © 2012 Elsevier B.V. All rights reserved.
doi:10.1016/j.bios.2012.02.039

a 3D cell population is complex. Thus, to make 3D cell structure on an electrode, we optimized and evaluated the gelatin condition between several types of sol–gels and A549 cancer cells and confirmed the reproducibility of electrical measurements for long-term monitoring. In addition, cytotoxicity test results showed that our 3D-cell-based biosensor monitoring can be an alternative method for high-throughput drug discovery screening.

2. Materials and methods

2.1. Cell cultures

A549 (human lung adenocarcinoma epithelial cell line) cells were cultured for continuous logarithmic-phase growth in a medium provided by the Roswell Park Memorial Institute (RPMI 1640, GIBCO, US) and 10% fetal bovine serum (FBS, GIBCO, US) in T-150 tissue culture flasks. Cells were incubated at 37 °C in 5% CO_2, 95% air humidified atmosphere. Culture medium was maintained fresh by changing every other day as needed.

2.2. Reagents and preparation of the three-dimensional cell chips

Alginic acid sodium salt (low viscosity, Sigma, US) was dissolved in sterile de-ionized distilled water to a concentration of 3% (w/v) solution at room temperature. After mixing 100 μL of 0.1 M $BaCl_2$ with 200 μL of 0.01% poly-L-lysine solution (PLL, Sigma, US), 1 μL of sterile $BaCl_2$–PLL mixture was spotted onto a gold electrode (Ø 1.6 mm, Dropsens, Spain) and totally dried. Next, after mixing the A549 cell suspension in 10% FBS-supplemented RPMI 1640 (GIBCO, US) with 3% alginate solution to a final concentration of 10^6 cells/mL in 1% alginate solution, 1 μL of the alginate-cells mixture was gelated on a gold electrode (Ø 1.6 mm, Dropsens, Spain) at 37 °C in 5% CO_2, 95% air humidified atmosphere.

Collagen I peptide-coupled mussel adhesive protein (0.5 mg/mL MAPTrix HyGel, Kollodis Biosciences, US) was diluted with phosphate-buffer saline (PBS, GIBCO, US) to a final concentration of 4.0 wt% solution (40 mg/mL). MAPTrix linker (Kollodis Biosciences, US) was diluted with phosphate-buffer saline to a final concentration of 6.0 wt% solution (60 mg/mL). And each solution was continuously diluted with phosphate-buffer saline twice until 0.50 wt% collagen, 0.75 wt% linker solution was obtained. After making various concentrations of collagen solutions (0.5 wt%, 1.0 wt%, 2.0 wt%, 4.0 wt%) and linker solutions (0.75 wt%, 1.5 wt%, 3.0 wt%, 6.0 wt%), each of these mixed, coupled solutions was gelated on a gold electrode (Ø 1.6 mm, Dropsens, Spain) at 37 °C in 5% CO_2, 95% air humidified atmosphere. And 1 μL of A549 cell spot (10^6 cells/mL) was seeded and cultured in porous 3D extracellular matrix structure consisting of the collagen gelated on the electrode.

Matrigel (BD Biosciences, US) was diluted with Dulbecco's phosphate buffered saline (DPBS, GIBCO, US) to a concentration of 12.5% solution at 4 °C. 1 μL of the cold matrigel–DPBS mixture was spotted onto gold electrodes (Ø 1.6 mm, Dropsens, Spain) to make a flat matrigel layer by drying. After mixing A549 cell suspension in 10% FBS-supplemented RPMI 1640 (GIBCO, US) with matrigel to make a final concentration of 10^6 cells/mL in 25% matrigel solution at 4 °C, 1 μL of the cold matrigel–cells mixture was gelated on a gold electrode (Ø 1.6 mm, Dropsens, Spain) at 37 °C in 5% CO_2, 95% air humidified atmosphere.

2.3. Pharmacological treatments

In order to confirm that cellular death was caused by drug treatments, cytotoxicity studies were performed by treating erlotinib (Tarceva, BioVision, US) (0–100 μM) to 3D cell chips for 72 h after stabilizing the cells gelated on the electrode for 1 day.

2.4. Electrochemical measurement and data analysis

Gold screen-printed electrodes (DropSens, Spain) of 2 mm^2 were used as disk-shaped working electrodes. The electrodes of the conventional three-electrode configuration have a gold counter and silver pseudo reference electrodes. After 1-day cell stabilization and 3-day cell culturing, electrochemical measurements were carried out by the electrochemical analyzer (model 1040, CHInstruments, US). Square wave voltammetry (SWV) was performed in a 0.5 mM $K_3Fe(CN)_6$ solution containing 10 mM KCl (electrolyte solution) in the potential range of −0.5–0.6 V with pulse amplitude of 25 mV and frequency of 50 Hz. Electrochemical measurements were executed with the ferrocyanide solution as the mediator that enhanced the electrochemical signal by producing an electron flow during the redox reactions between ferrocyanide and ferricyanide (Jeong et al., 2010).

All values in Figs. 4 and 5 are given as mean ± standard deviation (SD). The statistical significance of differences was evaluated by unpaired *t*-test using SigmaPlot software (SYSTAT, US). Data were considered statistically significant if the *p*-value was less than 0.01 (**) and 0.001 (***), which indicated that the SWV peak values for the condition of the cells remarkably increased compared to the condition without cells. In addition, all values in Fig. 6 are plotted as mean ± standard error of the mean (SEM) using Prism 4 (GraphPad, US).

2.5. Immunocytochemistry

In order to directly observe cellular death induced by drug treatment, live/dead cell staining was performed using a live/dead viability/cytotoxicity kit (Invitrogen, US). After cultures were rinsed once with Dulbecco's phosphate-buffered saline (D-PBS), 2 μM calcein AM and 4 μM ethidium homodimer (EthD)-1 working solution is added to the cultures. Calcein AM induced green fluorescence by reacting to the esterase in the inner cell membrane of viable cells. EthD-1 showed red fluorescence when it penetrated the damaged cell membranes of dead cells. In the drug test, after electrochemical measurement, live cell staining of the each electrode was carried out and the fluorescence intensity of live cells on the working electrode was measured by GenePix 4000B Microarray Scanner (Molecular Devices, US) in order to check the reliability of the electrochemical method. In addition, unlike the electrochemical method cell counting kit (CCK) was added to the cell–gel spot cultures in a 96-well plate to compare the results of electrochemical measurement with those of the previous routine cell assay method.

3. Results and discussion

3.1. Characterization of the electrochemical biosensor applying 3D cell culture

Electrochemical biosensors having an advantage of label-free have been used to electronically monitor cell activity in a culture. Interestingly, although most investigations have been done with 2D cultures, we could effectively measure cell signals in a 3D culture. Cells mixed with sol–gel were spotted on the working electrode, and gel–cells mixture was gelated on the gold electrode, as illustrated in Fig. 1. Faradaic impedance investigation can be effective in analyzing cell activity by measuring the changes of electron transfer resistances between biomaterials and electrodes (Katz and Willner, 2003). Therefore, electrical potential and current can be applied to cell-based systems to monitor biological activity in the fields

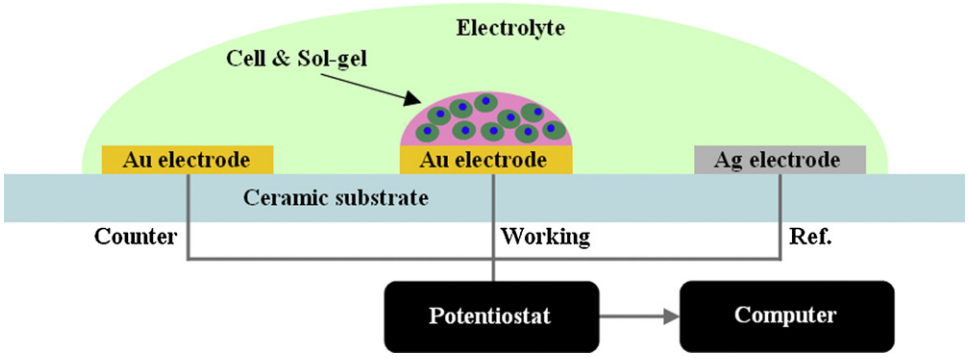

Fig. 1. Schematics of an electrochemical biosensor applying 3D cell culture. Cells mixed with sol–gel were spotted on the working electrode and the gel–cells mixture was gelated on a gold electrode.

of pharmacology, cell biology, and cytotoxicity. This is because variations of current according to the electrical potential applied to cells are useful information for obtaining functional information about the effect of a stimulus on living cells (Popovtzer et al., 2005).

Cancer cells in 3D show a different morphology than in 2D. While one layer of cells is observed in a 2D cell culture coated with poly-L-lysine, which adopt an unnatural spread morphology (Fig. 2(A)), cells in a 3D cell culture mixed with 25% matrigel had a clustered, rounded morphology, as shown in Fig. 2(B), which is reminiscent of tumors in vivo (Gurski et al., 2009; Feder-Mengus et al., 2008). According to other research, 3D cell cultures are composed of not only proliferating cells, and non-proliferating viable cells, but also necrotic cells, which resemble multiple phenotypes. 2D cultures are not limited by mass transport because they are more homogeneous. However, 3D cultures have transport limitations mimicking an in vivo response against external compounds due to the restriction of accessibility and cellular heterogeneity (Dhiman et al., 2005). A 3D cell culturing, therefore, could be an alternative method for evaluating different anticancer drugs in lung cancer. For these reasons, 3D culture is a model system for understanding the regulation of cancer cell proliferation and for evaluation of different anticancer drugs (Bissell et al., 2003; Padron et al., 2000).

In a 2D culture, as the cells proliferate on the electrode, the peak value of current decreases because the impedance of the electrode coated with the cells becomes higher than that of the electrode not coated with any biomaterials, as shown in Fig. 3(A and B). In other words, the effect of binding events on electron transfer resistance depends on the character of the target molecules. The binding of cells on the electrode reduces current because a cell layer interferes in the electron flow between a redox molecule and the electrode (Xing et al., 2006; Strehlitz et al., 2008).

On the other hand, the signal change in a 3D culture could be the result of something different. In Fig. 3(C), the electrical signal is very weak because the gel acts as a type of non-conductor. However, if there are live cells in the gel, there would be a meaningful difference of signals between the conditions in Fig. 3(C and D). This means that the live cells might allow many ions to pass to the electrode. Although basically cells are considered non-conductors consisting of cell membranes, gap junctions of cells act as channels through the cell membrane that allow electrical connections among neighboring cells. When cells are electrically stimulated, gap junctions of the cells effectively connect electrically to the cells. As a result, the sensitivity of cells by externally applying electrical field increases and cells may act as a conductor for a short time by considerable biochemical and biophysical changes (Knedelitschek et al., 1994; Cooper, 1984; Fear and Stuchly, 1998; Kotnik and Miklavčič, 2000). Therefore, we assumed that as the number of cells is increased, the electrical signal would also be increased in a 3D culture. However, although the signal difference may be meaningful, it would still have limited use in a drug test if the value of the signal

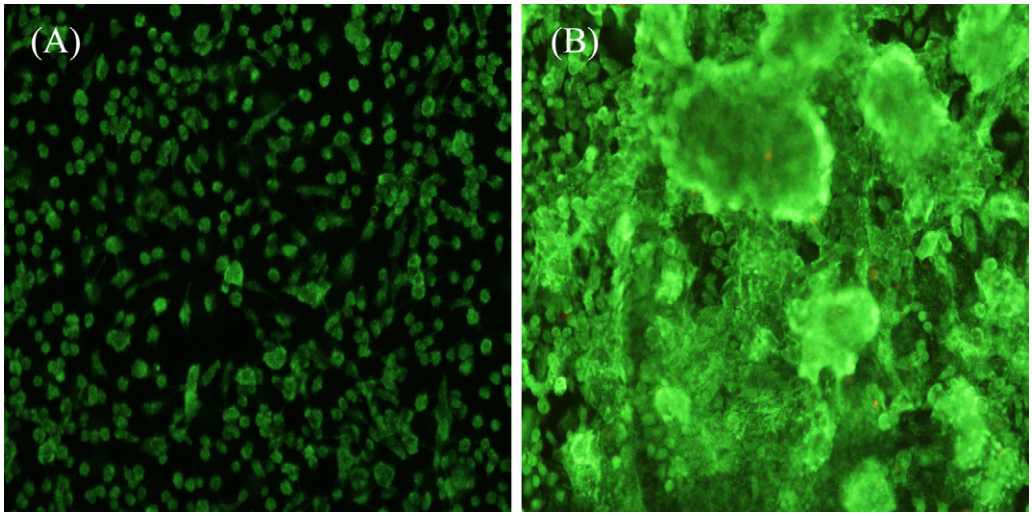

Fig. 2. Comparison of 2D culture and 3D culture. (A) In 2D culture, cells are formed as a layer on the plate. (B) 3D cells mixed with matrigel were formed in a clustered morphology.

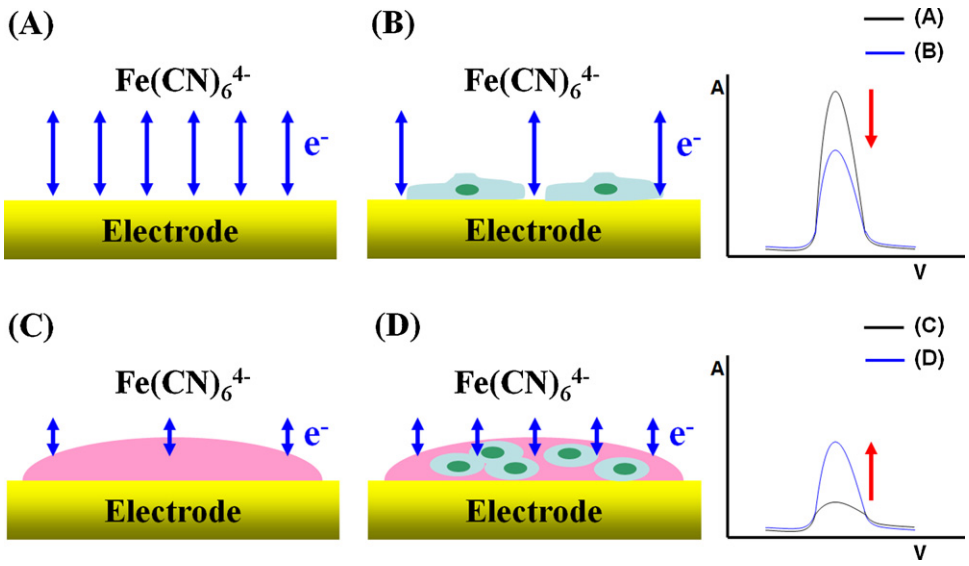

Fig. 3. Different aspects of electrical signal between 2D culture and 3D culture. (A) Electrode only. (B) 2D culture on the electrode. (C) Gel only on the electrode. (D) 3D culture in the gel on the electrode.

difference is small. Thus, experimental conditions have to be optimized not only to overcome this limited use but also to verify the above hypothesis.

3.2. Optimization for enhancement of signal effectiveness

Fig. 4 displays the current values according to the type of sol–gel and the change of concentrations of sol–gel. Each current value indicates the peak value of the electrical signal measured by square wave voltammetry according to the measurement procedure of the cell based biosensor. SWVs were carried out in 0.5 mM $K_3Fe(CN)_6$ solution containing 10 mM KCl in the voltage range of −0.5–0.6 V. In this work, SWV was mainly used to measure electrochemical changes because SWV has rapid scan rates and because its peak-shaped voltammograms have excellent sensitivity to and filtering ability of background currents. This is because the SWV suppresses capacitive currents, which induce charge effects on the bio molecule layer (Zhang and Millero, 1994; Kim et al., 2007).

In the alginate case, the 0.25% alginate condition and the 1% alginate condition indicated that the SWV peak values for the condition of cells were considerably increased from 2.17 ± 0.05 μA to 2.70 ± 0.04 μA and from 2.07 ± 0.04 μA to 2.92 ± 0.04 μA, respectively ($n = 3$, $^{**}p < 0.01$) as shown in Fig. 4(A). On the other hand, collagen conditions did not show significant results because most differences of the peak values between conditions of cells and no cells were within 5 μA (Fig. 4(B), $n = 3$). In the matrigel case, however, the 25% matrigel condition showed that the SWV peak values of the condition with cells were remarkably increased from 1.95 ± 0.04 μA to 3.09 ± 0.07 μA, as shown in Fig. 4(C) ($n = 3$, $^{***}p < 0.001$). This indicated that under the 25% matrigel condition the SWV peak values for the condition of cells were most noticeably increased compared to the condition without cells. This result provided a significant experimental condition in drug treatment test. This is because the bigger difference of the peak values between conditions of cells and no cells in optimized conditions was shown, the more accurate IC_{50} value of a drug could be derived from a dose–response curve.

3.3. Measurement of cell viability according to cell seeding density

Under the same 25% matigel condition, the SWV signals according to differences of initial cell seeding density were measured, as shown in Fig. 5(A). The SWV peak values for the conditions with no cells (25% matrigel only) and with cells at 10^6 cells/mL in the 25% matrigel conditions were 1.93 μA and 3.28 μA, respectively. Fig. 5(B) indicated that there was also a trend in which the peak values of SWV increased according to the increase of cell seeding density ($n = 3$). These differences of SWV signals according to the cell density might be caused by the difference in the ratio of the number of cells to matrigel in the same volume on the working electrode. Since the impedance of the matrigel-only electrode is higher than that of the matrigel-mixed cells electrode as mentioned the above.

When the number of cells is increased by cells proliferation, cell death can occur (Sun et al., 2002). Thus, it is a necessity to identify which level of cell density would make a significant signal between cells and the electrode without cell death. An image of each cell staining was recorded at the 4th day (1 day cell stabilizing and 3 days cell culturing) after seeding the cells in 25% matrigel based on the result of Fig. 5. As depicted in Fig. 5(C), green and red indicate live cells and dead cells, respectively. From 0 to 10^6 cells/mL, the parts showing live cells showed a trend in which the cell density increases, whereas the parts showing dead cells did not show any significant difference in cell density. Even in the condition of primary seeding density of 10^6 cells/mL, few dead cells were observed, as shown in Fig. 5(C).

3.4. Drug dose response on the electrochemical biosensor applying 3D cell culture

In order to confirm the feasibility of application of the electrochemical biosensor for cytotoxicity assay on 3D cell culture, we have investigated the drug efficacy of erlotinib, which is a representative lung cancer drug. 3D cells were spot gelated on the electrode at density of 10^6 cells/mL in 25% matrigel. And cytotoxicity studies were performed by treating erlotinib of various concentrations

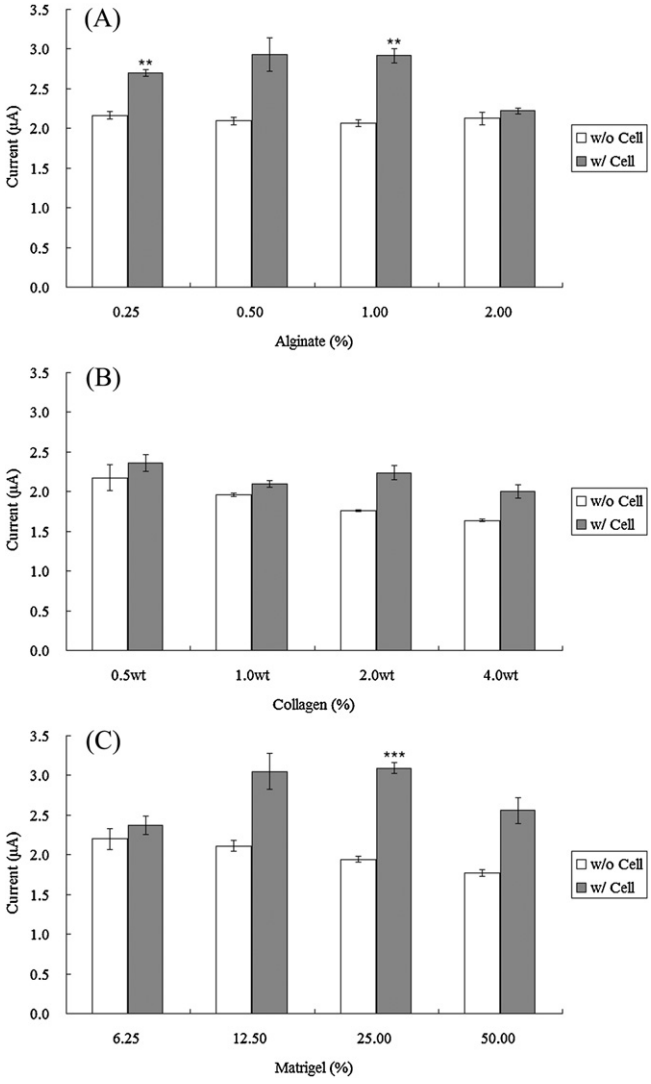

Fig. 4. Comparison of SWV peak values between cell-included gel and only gel according to the type of sol–gel and concentrations. (A) Alginate condition. (B) Collagen condition. (C) Matrigel condition. $^{**}p < 0.01$, $^{***}p < 0.001$ when compared to the each control group respectively.

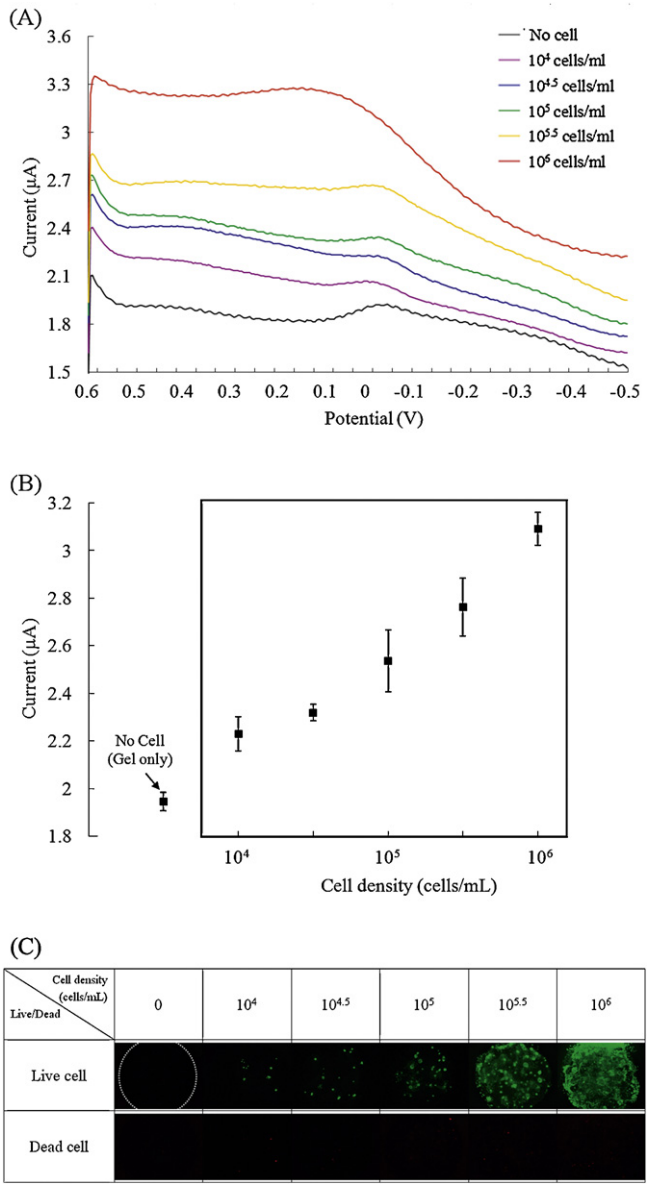

Fig. 5. Change of electrical current and fluorescence intensity according to cell density (25% Matrigel). (A) Current values of SWV are different depending on the condition of cell seeding density. (B) A linear graph of peak value of current according to cell seeding density. (C) Fluorescent stain of cell on the electrode. Each cell was pictured at the DIV 4 after cell seeding. Green: live cells, red: dead cells. Even in 10^6 cells/mL condition, cells were fine cultured without cell death. The white circle indicates the region of working electrode. (For interpretation of the references to color in this figure legend, the reader is referred to the web version of the article.)

(0–100 μM) to 3D cell chips in culture media for 72 h after stabilizing the cells gelated on the electrode for 1 day. Current values of SWV were measured differently following the density of the remaining live cells. Using these current values, cell viability was plotted, as shown in Fig. 6(A).

Cell viability can be defined as follows:

$$\text{Cell viability}(\%) = \frac{I_2 - I_0}{I_1 - I_0} \times 100 \quad (1)$$

Here, I_0 indicates the condition of matrigel only and I_1 indicates the condition of control cells mixed with matrigel. And I_2 indicates the condition of drug treatments to cells mixed with matrigel. As shown in Fig. 6(A–C), cell viability decreased with the increase of erlotinib concentration. The IC_{50} of a drug was determined by constructing a dose–response curve. The IC_{50} value of erlotinib applied to A549 cells was 17.54 μM ($n = 8$; $R^2 = 0.86$) (Fig. 6(A)). To explain, the current value of SWV could increase according to the increase of the number of cells in matrigel, thus I_2 values decreased because the number of remaining live cells decreased by drug toxicity as drug concentrations increased. Additionally, in order to check the reliability of the electrochemical method, the fluorescence intensity of live cells on the working electrode was measured by an optical system. As shown in Fig. 6(B), the values of the fluorescence intensity not only decreased with the increasing of erlotinib concentration, but also were considerably similar to the dose–response curve in Fig. 6(A). IC_{50} value determined from the plot of a dose–response curve measured by the optical system was 8.76 μM ($n = 4$; $R^2 = 0.81$) (Fig. 6(B)).

Although the IC_{50} value of erlotinib in this experiment was comparatively higher than that in previous results of the 2D cell culture, this result corresponded with previous data in which A549 cell was classified as erlotinib resistant when IC_{50} value was more than 2 μM (Giovannetti et al., 2008; Li et al., 2007; Ikeda et al., 2011). And more importantly, this result explains that 3D culturing increased drug resistance (Tung et al., 2011; Lee et al., 2008b; dit Faute et al., 2002).

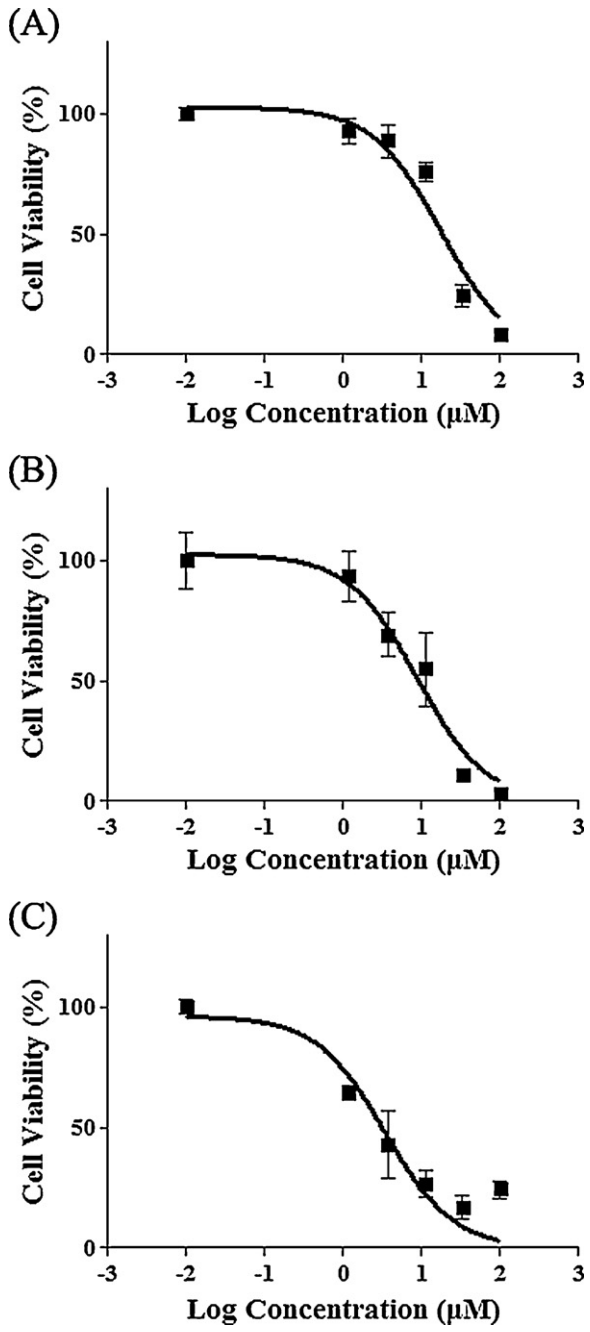

Fig. 6. Comparison of dose response curves of cell viability according to drug concentrations (A) electrochemical measurement (B) optical measurement (C) cell count kit (CCK).

In order to compare the results of the new electrochemical method for 3D cell culture with those of the conventional cell assay method, cell counting kit was applied to cell–gel spot cultures on the cell culture plate under the same condition as the 3D cell chip. As a result, cell viability was decreased following the increase of erlotinib concentrations. And Fig. 6(C) indicates that IC_{50} value determined from the plot of a dose–response curve was 4.39 μM ($n = 4$; $R^2 = 0.75$). Based on these results, although some aspects among three graphs in Fig. 6 were not exactly the same, the overall trend of decrease seemed quite similar. And more importantly, each IC_{50} value of erlotinib treated on A549 cell was shown to be in the similar range in that both values were over 2 μM. For these reasons, our work suggests a useful method for monitoring 3D cell response in real time. Also, these results show the feasibility of application of the new electrochemical biosensor for cytotoxicity assay in the investigation of 3D cell response to drug compounds.

4. Conclusion

We optimized the condition of gelation between several types of sol–gel and A549 cancer cells to enhance signal effectiveness and verified the reproducibility of electrical measurement for long-term monitoring by an electrochemical biosensor applying 3D cell culture. In addition, we confirmed the feasibility of application of the electrochemical biosensor for analysis of 3D cell culture to cytotoxicity assay by investigating the drug efficacy of erlotinib with the biosensor. Thus, our work provides a useful means not only to observe 3D cell responses in real time, but also to investigate drug responses by high-throughput cytotoxicity assay.

Acknowledgments

I am thankful to all my colleagues including SH Yi in AMD lab, HS Lee, KH Kim in SMC who supported me in any respect during the completion of the project.

References

Albers, J., Grunwald, T., Nebling, E., Piechotta, G., Hintsche, R., 2003. Anal. Bioanal. Chem. 377 (3), 521–527.
Andreescu, S., Sadik, O.A., 2005. Methods 37 (1), 84–93.
Bissell, M.J., Rizki, A., Mian, I.S., 2003. Curr. Opin. Cell Biol. 15 (6), 753–762.
Boero, C., Carrara, S., Vecchio, G.D., Calzà, L., Micheli, G.D., 2011. Sens. Actuators B 157 (1), 216–224.
Cooper, M., 1984. J. Theor. Biol. 111, 123–130.
Dhiman, H.K., Ray, A.R., Panda, A.K., 2005. Biomaterials 26 (9), 979–986.
Ding, L., Du, D., Wu, J., Ju, H., 2007. Electrochem. Commun. 9 (5), 953–958.
dit Faute, M.A., Laurent, L., Ploton, D., Poupon, M.F., Jardillier, J.C., Bobichon, H., 2002. Clin. Exp. Metastasis 19 (2), 161–168.
Fear, E.C., Stuchly, M.A., 1998. IEEE Trans. Biomed. Eng. 45 (10), 1259–1271.
Feder-Mengus, C., Ghosh, S., Reschner, A., Martin, I., Spagnoli, G.C., 2008. Trends Mol. Med. 14 (8), 333–340.
Giovannetti, E., Lemos, C., Tekle, C., Smid, K., Nannizzi, S., Rodriguez, J.A., Ricciardi, S., Danesi, R., Giaccone, G., Peters, G.J., 2008. Mol. Pharmacol. 73 (4), 1290–1300.
Gurski, L.A., Jha, A.K., Zhang, C., Jia, X., Farach-Carson, M.C., 2009. Biomaterials 30, 6076–6085.
Ikeda, R., Vermeulen, L.C., Lau, E., Jiang, Z., Kavanaugh, S.M., Yamada, K., Kolesar, J.M., 2011. Oncol. Lett. 2 (1), 91–94.
Jeong, S.H., Kim, C.S., Yang, J., 2010. BioChip J. 4 (2), 141–147.
Jeong, S.H., Lee, S.H., Jun, S.B., Kim, S.J., Park, T.H., 2009. Electrophoresis 30, 3283–3288.
Katz, E., Willner, I., 2003. Electroanalysis 15, 913–947.
Kaya, T., Torisawa, Y., Oyamatsu, D., Nishizawa, M., Matsue, T., 2003. Biosens. Bioelectron. 18 (11), 1379–1383.
Kim, Y.S., Jung, H.S., Matsuura, T., Lee, H.Y., Kawai, T., Gu, M.B., 2007. Biosens. Bioelectron. 22 (11), 2525–2531.
Knedelitschek, G., Noszvai-Nagy, M., Meyr-Waarden, H., Schimmelpfeng, J., Weibezahn, K.F., Dertinger, H., 1994. Radiat. Environ. Biophys. 33, 141–147.
Kotnik, T., Miklavčič, D., 2000. Bioelectromagnetics 21, 385–394.
Lee, J., Cuddihy, M.J., Kotov, N.A., 2008a. Tissue Eng. Part B: Rev. 14 (1), 61–86.
Lee, M.Y., Kumar, R.A., Sukumaran, S.M., Hogg, M.G., Clark, D.S., Dordick, J.S., 2008b. Proc. Natl. Acad. Sci. U.S.A. 105 (1), 59–63.
Li, T., Ling, Y.H., Goldman, I.D., Perez-Soler, R., 2007. Clin. Cancer Res. 13 (11), 3413–3422.
Mehrvar, M., Abdi, M., 2004. Anal. Sci. 20, 1113–1126.
Mueller-Klieser, W., 1997. Am. J. Physiol. 273 (4 Pt. 1), C1109–C1123.
Padron, J.M., van der Wilt, C.L., Smid, K., Smitskamp-Wilms, E., Backus, H.H., Pizao, P.E., Giaccone, G., Peters, G.J., 2000. Crit. Rev. Oncol. Hematol. 36 (2–3), 141–157.
Petersen, O.W., Rønnov-Jessen, L., Howlett, A.R., Bissell, M.J., 1992. Proc. Natl. Acad. Sci. U.S.A. 89 (19), 9064–9068.
Popovtzer, R., Neufeld, T., Biran, D., Ron, E.Z., Rishpon, J., Shacham-Diamand, Y., 2005. Nano Lett. 5 (6), 1023–1027.
Rodrigues, N.P., Sakai, Y., Fujii, T., 2008. Sens. Actuators B 132 (2), 608–613.
Strehlitz, B., Nikolaus, N., Stoltenburg, R., 2008. Sensors 8, 4296–4307.
Sun, C.F., Haven, T.R., Wu, T.L., Tsao, K.C., Wu, J.T., 2002. Clin. Chim. Acta 321 (1–2), 55–62.
Tung, Y.C., Hsiao, A.Y., Allen, S.G., Torisawa, Y., Ho, M., Takayama, S., 2011. Analyst 136, 473–478.
Xing, J.Z., Zhu, L., Gabos, S., Xie, L., 2006. Toxicol. In Vitro 20 (6), 995–1004.
Yang, S.T., Zhang, X., Wen, Y., 2008. Curr. Opin. Drug Discov. Dev. 11 (1), 111–127.
Yue, X., Drakakis, E.M., Lim, M., Radomska, A., Ye, H., Mantalaris, A., Panoskaltsis, N., Cass, A., 2008. IEEE Trans. Biomed. Circuits Syst. 2 (2), 66–77.
Zhang, F., Tian, J., Wang, L., He, P., Chen, Y., 2011. Sens. Actuators B 156 (1), 416–422.
Zhang, J.Z., Millero, F.J., 1994. Anal. Chim. Acta 284 (3), 497–504.